ELSEVIER

Generation and propagation of infrasonic airwaves from volcanic explosions

J.B. Johnson [1],*

Geophysics Program, University of Washington, Seattle, WA, USA

Abstract

Analysis of infrasonic pressure waves generated by active volcanoes is essential to the understanding of volcanic explosion dynamics. Unlike seismic waves propagating in the earth, infrasonic airwaves offer a relatively unfiltered representation of source motions at the vent during an eruption. Time-varying acoustic propagation filters caused by changeable atmospheric conditions are minimal for microphones deployed at intermediate distances (< 5 km from the vent). Thus the recorded excess pressure time series directly reflects the impulsivity of the degassing source at the vent. In the most simple experiments, infrasound monitoring is valuable for differentiation of subsurface seismicity from the seismicity associated with an eruption. In other instances, infrasound monitoring may be used in conjunction with seismic monitoring to understand the style of eruption and information about the physical source processes and source location. This manuscript is an introductory overview of the generation and propagation of volcanic infrasound. An analysis of infrasonic records generated from five volcanic case studies is provided in an accompanying article [Johnson et al., J. Volcanol. Geotherm. Res., in press].
© 2002 Elsevier Science B.V. All rights reserved.

1. Introduction

Even when an active volcano is obscured by clouds, 'detonations', 'booming', 'cracking', and 'whooshing' noises can indicate the eruption of gas and solid material from a vent. Richards (1963) recorded audible acoustic noises from a suite of volcanoes with activities ranging from Hawaiian and Strombolian to Vulcanian and ac-

knowledged that volcanic sources generate substantial low-frequency acoustic energy. More recently, other investigators have deployed microphones sensitive to infrasonic frequencies (below 20 Hz) in the vicinity of actively degassing volcanoes. These experiments include: Tolbachik and Klyuchevskoi (Firstov and Kravchenko, 1996), Stromboli (Vergniolle et al., 1996), Unzen (Yamasato, 1998), Sakurajima (Garces et al., 1999), Arenal (Hagerty et al., 2000), Erebus (Rowe et al., 2000), Karymsky and Sangay (Johnson and Lees, 2000), and previously unpublished records from Tungurahua and Pichincha presented in an accompanying article (Johnson et al., in press).

[1] Present address: Hawaii Institute of Geophysics and Planetology, University of Hawaii, Manoa, HI, USA.

* Tel.: +1-808-956-3149; Fax: +1-808-956-6322.
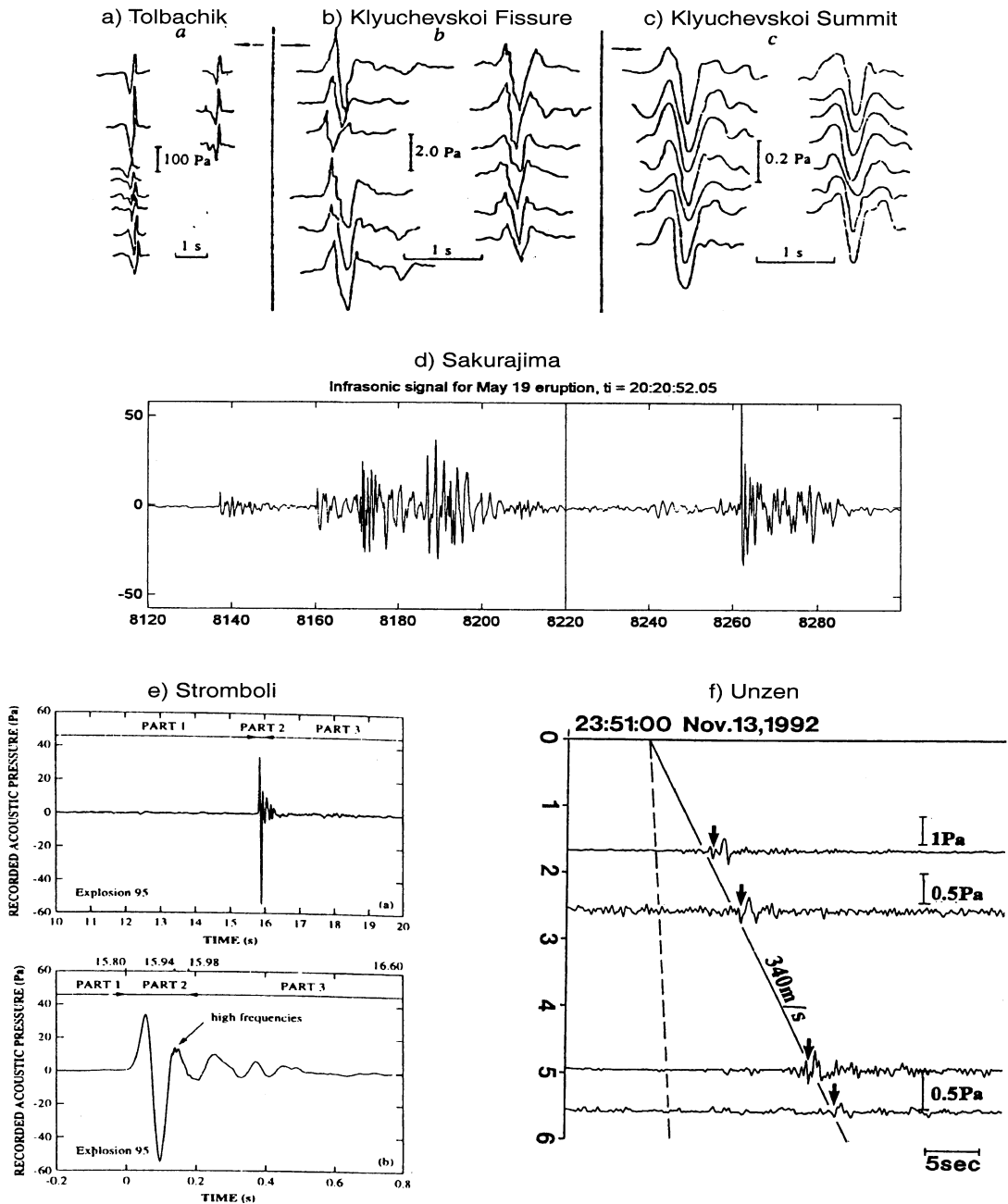*E-mail address:* jbj@higp.hawaii.edu (J.B. Johnson).

Fig. 1. Some examples of volcanic infrasound. (a) Tolbachik (note that the time axis is reversed), (b,c) Klyuchevskoi (Firstov and Kravchenko, 1996), (d) Sakurajima (Garces et al., 1999), (e) Stromboli (Vergniolle et al., 1996), (f) Unzen (Yamasato, 1998), (g,h) Arenal (Hagerty et al., 2000), (i) Erebus (Rowe et al., 2000), (j,k) Karymsky (Johnson and Lees, 2000), and (l) Sangay (Johnson and Lees, 2000). Microphone epicentral distances are listed in Table 1.

g,h) Arenal

i) Erebus
Jan 10, 1998 05:36 UTC

Acoustic
± 50 Pa

E1LI

TIME (SECONDS)

j,k) Karymsky

Karymsky Simple Impulse Event (1997:234:07:01)

Karymsky Chugging Event (1997:233:15:23)

l) Sangay

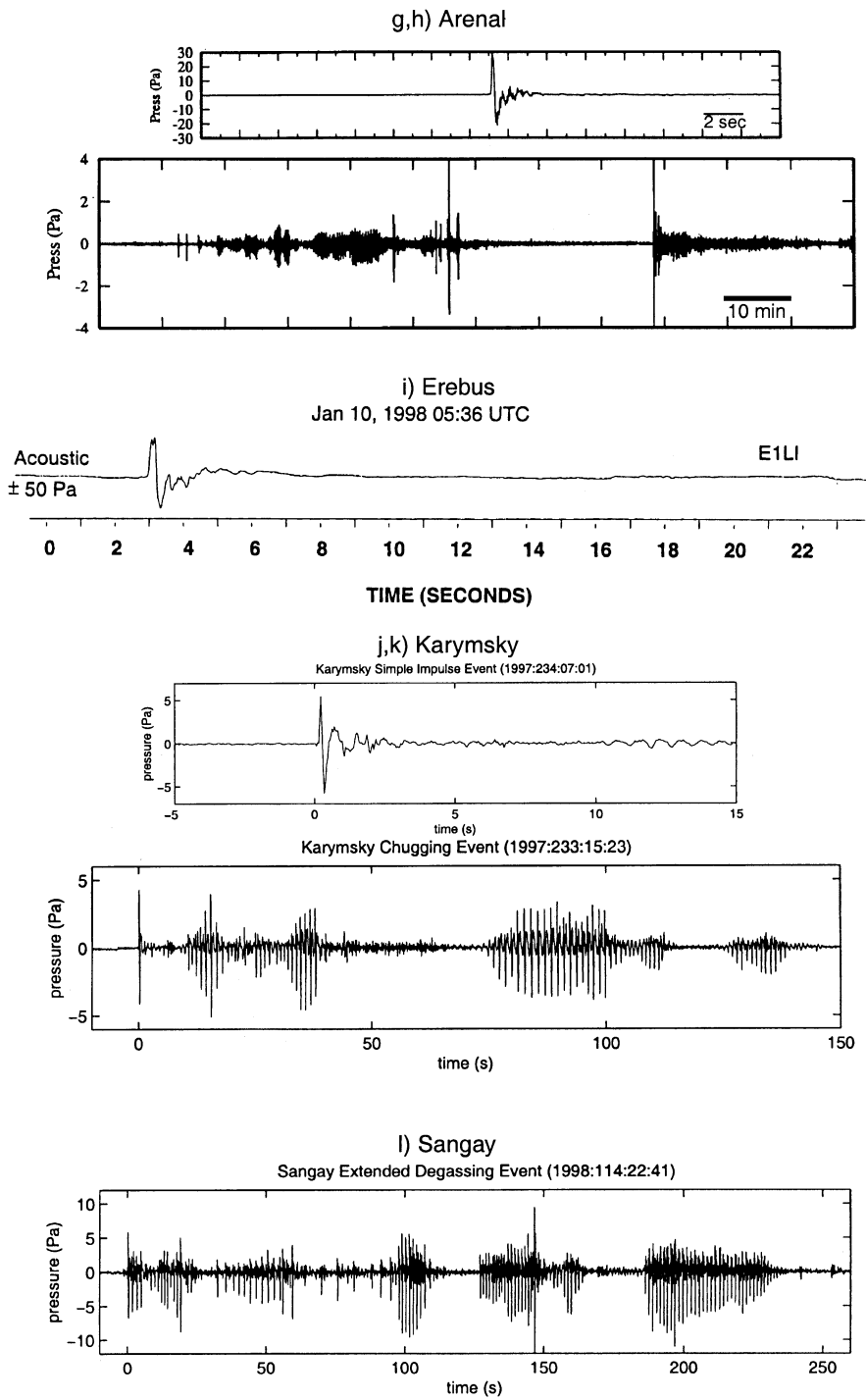Sangay Extended Degassing Event (1998:114:22:41)

Fig. 1 (*Continued*).

Infrasound records from a suite of different volcanoes (Fig. 1) reveal varied and distinct degassing behaviors. In many instances, most notably at Tolbachik, Klyuchevskoi, Stromboli, Erebus, and in certain explosions from Arenal and Karymsky (Fig. 1a–c,e,g,i,j), infrasonic waveforms consist solely of a single impulsive compression followed by a more lengthy rarefaction. In other instances, most notably at Sakurajima, Arenal, Karymsky, and Sangay (Fig. 1d,h,k,l), pressure traces have a complex coda lasting several minutes indicative of continued degassing. Nevertheless, many of these extended degassing events also begin with the characteristic impulsive compressional onset. The examples in Fig. 1 are provided as an overview of infrasound signals generated by different volcanoes and are not necessarily representative of typical degassing behavior at each of the volcanoes.

Infrasonic pressure traces are time histories of atmospheric pressure pertubations (ΔP) relative to background atmospheric pressure. This excess pressure is usually very small compared to ambient atmospheric pressure ($\sim 10^5$ Pa). Thus much volcanic infrasound can be treated as linear elastic waves rather than non-linear shock waves. The infrasonic traces in Fig. 1 that are recorded several km from the explosion source have peak excess pressures ranging from 10^1 Pa to 10^2 Pa. Although these low-frequency signals are inaudible to humans, conversion to the more recognizable units of sound pressure level (SPL) can sometimes be illustrative:

$$\text{SPL} = 20\log\left(\frac{\Delta P}{2 \times 10^{-5}\text{Pa}}\right) \tag{1}$$

Thus an excess pressure of 10^1 Pa (a typical infrasound amplitude recorded 1 km from a Strombolian source) corresponds to an SPL of 115 dB. In the audible frequency band, this SPL is the noise equivalent of a pneumatic riveter (Truax, 1978).

2. Acoustic energy

At Karymsky and Sangay Volcanoes, audible sounds generated during eruption rarely exceed an SPL comparable to street traffic (80 dB) several km from the vent (author's observation). Vergniolle et al. (1996) also estimate that explosions at Stromboli Volcano are about 30 dB 'softer' in the audible band than in the infrasonic band. Because acoustic energy scales with the square of acoustic excess pressure (Truax, 1978), the 30 dB difference in SPL indicates three orders of magnitude difference in acoustic energy. We target infrasonic frequencies during volcano monitoring because the acoustic intensity is greatest in this band. Much volcanic infrasound appears to be dominated by frequencies between 0.5 Hz and 10 Hz (Garces and McNutt, 1997; Hagerty et al., 2000; Johnson and Lees, 2000; Rowe et al., 2000), which is within the typical bandwidth of interest for volcanic seismicity. This allows for convenient simultaneous seismo-acoustic recording with a single datalogger or telemetry site.

For a source which radiates acoustic waves spherically, the total acoustic energy is proportional to the time-integrated squared excess pressure trace. For hemispherically radiating infrasound (see Appendix):

$$E_{\text{acoustic}} = \frac{2\pi r^2}{\rho_a c} \int \Delta P^2 dt \tag{2}$$

where r is the distance between source and receiver (m); ρ_a is the air density (1.189 kg/m^3 at standard temperature and pressure (STP)); and c is the sound speed (343 m/s at STP).

Though radiated acoustic energy is typically only a very small portion of a volcano's overall eruptive energy budget (McGetchin and Chouet, 1979), it is a useful parameter for characterizing the integrated acoustic intensity over the duration of an eruption. Table 1 provides energy estimates based upon Eq. 2 for the waveforms displayed in Fig. 1.

3. Volcanic explosion source

The commonest source of volcanic infrasound is the atmospheric pertubation caused by the explosive outflux of volcanic volatiles. During eruptions, gas flux through a vent can range from 10^1 kg/s for Strombolian bursts to 10^8 kg/s for Plinian

Table 1
Summary of Parameters for Infrasonic Signals from Fig. 1

Volcano name, magma chemistry, and infrasonic waveform characteristics	Distance of microphone from source (km)	Peak excess pressure of waveform (Pa)	SPL at 100 m[a] (dB)	Estimated explosion duration[b] (s)	Acoustic energy estimated from trace data[c] (MJ)
(a) Tolbachik, basalt, single pulses	1.9–2.6	100	160	2	1×10^2
(b) Klyuchevskoi fissure, basalt, single pulses	12.2	2	142	3	2×10^0
(c) Klyuchevskoi summit, basalt, single pulses	14.6	0.2	123	3	2×10^{-2}
(d) Sakurajima, andesite, extended degassing	~ 3.0	4	136	$\sim 10^4$	4×10^2
(e) Stromboli, basalt, single pulse	0.3	50	136	0.5	1×10^{-1}
(f) Unzen, dacitic dome, emergent, low amplitude	1.7	1	119	~ 5	1×10^{-2}
(g) Arenal 1, andesite, single pulse	~ 2	30	150	3	1×10^1
(h) Arenal 2, andesite, extended duration explosion	~ 2	4	132	$\sim 10^3$	3×10^1
(i) Erebus, phonolite, single pulse	0.7	50	145	4	4×10^0
(j) Karymsky 1, andesite, single pulse	1.6	5	132	4	2×10^{-1}
(k) Karymsky 2, andesite, series of pulses	1.6	5	132	$\sim 10^2$	3×10^0
(l) Sangay, basaltic andesite, series of pulses	2.2	10	141	$\sim 10^2$	2×10^1

[a] Equivalent SPL for peak excess pressures reduced to 100 m epicentral distance, assuming an inverse relationship between pressure amplitude and distance.

[b] Time duration of signal that remains above background noise level (note that background noise has variable amplitude at different volcanoes).

[c] Acoustic trace energy calculated according to Eq. 2, assuming hemispherical radiation.

columns (Newhall and Self, 1982). However, infrasonic data has traditionally been collected at volcanoes with VEI I and VEI II eruptions which provide frequent, repetitive explosions and relatively safe access for instrument deployment. Infrasound generation at the Strombolian end of the eruption spectrum is relatively easy to model for the following reasons: (1) a point source approximation is appropriate, (2) infrasound sources are primarily generated at the conduit/atmosphere interface and not within a convecting column, (3) the bulk of the elastic wave energy is produced prior to the mixing of magmatic and atmospheric gases, (4) ejection velocities are subsonic. A point source approximation will not be appropriate for larger eruption plumes (Vulcanian and Plinian eruptions), where infrasound can be generated from a diffuse volume with a dimension greater than infrasonic wavelengths.

Though models have been proposed which invoke acoustic radiators imbedded in a fluid-filled conduit (Garces and McNutt, 1997), the consensus among many researchers is that the fundamental source of infrasound at VEI I and VEI II volcanoes is the rapid release of pressurized gas at the free surface. Yamasato (1997) calculated radiated acoustic pressures for two types of sources at Unzen Volcano (ground dislocations and volumetric gas expansions) and concluded that reasonable ground dislocations were not large enough to produce the observed infrasonic signals. Other investigators (Firstov and Krav-

chenko, 1996; Vergniolle et al., 1996; Rowe et al., 2000; Johnson and Lees, 2000) use visual observations to substantiate that the primary compressional infrasonic pulse is coincident with rapid gas expansion from the vent.

Some very energetic volcanic eruptions also generate atmospheric pressure pertubations with very long periods (greater than 270 s) that are propagated by buoyancy forces (Beer, 1974). These acoustic gravity waves are observed in the far-field in association with extremely large movements of air parcels such as the 1980 Mount St. Helens eruption (Mikumo and Bolt, 1985) or the 1992 Pinatubo eruption (Tahira et al., 1996). They are not readily observed in association with VEI I and II eruptions where heat injection into the atmosphere is relatively small (Wilson et al., 1978).

Acoustic pressure traces in the near-infrasound bandwidth (0.1–20 Hz) are valuable because they reveal information about physical motions at the vent. As with seismic data, near-infrasound is a linear convolution of a source function, a Green's function, and instrument response. However, unlike seismic propagation filters in the earth, atmospheric propagation filters are relatively benign. They tend not to distort acoustic waveforms significantly because the atmosphere does not support shear waves and the atmosphere is largely devoid of structures which scatter, attenuate, or reflect acoustic waves. In some cases, however, reflections of the atmosphere/ground interface, such as crater wall echoes (Johnson et al., in press), may be responsible for complexities in infrasonic pressure waveforms. At epicentral distances common during the deployment of infrasonic stations, an atmospheric velocity structure that is dependent upon temperature and wind can influence acoustic arrival times and signal strength (see Section 4). These effects must be considered when using infrasound records to locate explosion sources and when assessing the intensity of an eruption.

Deconvolution of the instrument response from infrasonic waveforms is relatively uncomplicated as many modern pressure transducers and electret condenser microphones possess nearly flat sensitivities and linear phase responses in the frequencies of interest. For electret condenser micro-

phones with known low-frequency roll-off, instrument responses may be removed by applying digital transfer functions (Johnson et al., in press).

A linear approximation is suitable for infrasound sources with pressure pertubations which are infinitesimal with respect to the ambient atmospheric pressure. Assuming a point source in a homogeneous medium, the restoring force in the atmosphere is proportional to particle displacement. Acoustic compressional waves propagate elastically according to the wave equation for spherical waves (Jensen et al., 1994):

$$\nabla^2(\Delta P) - \frac{1}{c^2}\frac{\partial^2}{\partial t^2}(\Delta P) = -F(t)\delta(r) \tag{3}$$

where $F(t)$ is the effective force function.

The solution to the inhomogeneous wave equation can then be written in the form (Lay and Wallace, 1995):

$$4\pi r\Delta P = -F\left(t - \frac{r}{c}\right) \tag{4}$$

The sound speed is (Ford, 1970):

$$c = \sqrt{\frac{E}{\rho_a}} = \sqrt{\gamma RT} \approx \sqrt{402.8T} \tag{5}$$

where E is the bulk modulus (1.4×10^5 Pa at STP); γ is the heat capacity ratio (1.4 at STP); R is the gas constant (287 J/kg/K); and T is the temperature in K.

In the atmosphere, sound speed is directly proportional to the square root of temperature (Ford, 1970). In the lower atmosphere (troposphere), acoustic waves may propagate as slowly as 306 m/s (at −40° C) and as fast as 355 m/s (at +40° C).

For a simple acoustic source, the effective force function is equal to the rate of change of flux (mass outflow) from the source (Lighthill, 1978). According to the linear theory of sound, excess pressure due to an acoustic source radiating into a halfspace is then (Lighthill, 1978):

$$\Delta P = \left(\frac{1}{2\pi r}\right)\left[\frac{dq(t - r/c)}{dt}\right] \tag{6}$$

where $q(t)$ is the mass flux from a point source.

Fig. 2 shows a synthetic acoustic pressure trace calculated according to Eq. 6.
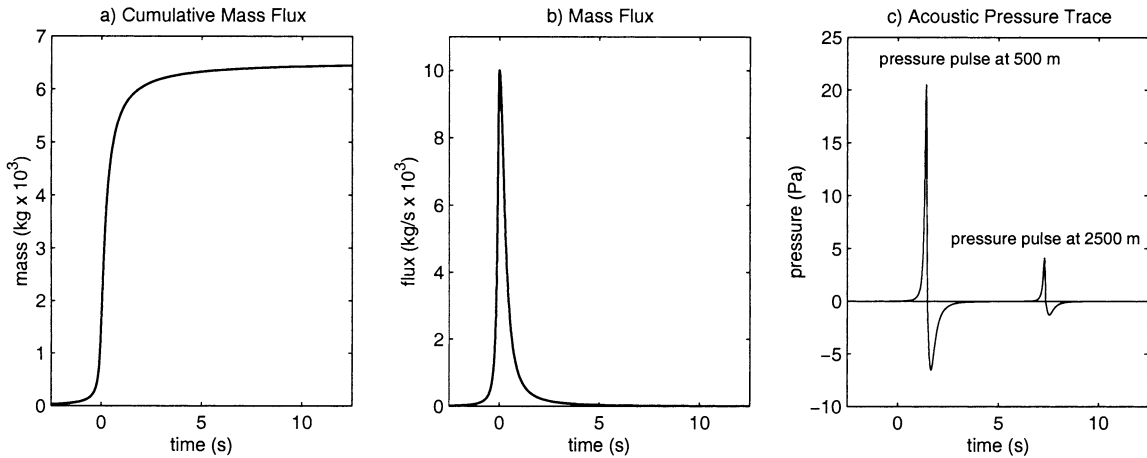
Fig. 2. Gas mass flux and synthetic infrasonic pulse. The generation of a transient acoustic pressure pulse from a point source gas release into a halfspace. The arbitrary mass flux function is intended to represent a rapid degassing onset followed by more gradual tapering. (a) Cumulative gas flux (integrated mass flux history) for an impulsive explosion. (b) Time history of the mass flux (the arbitrary mass flux function is described by $10000/(t^2+0.01)$ for $t<0$ and $10000/(t^2+0.1)$ for $t>0$). (c) Transient pressure pulses calculated at 500 m and 2500 m from the vent (according to Eq. 6) assuming a homogeneous STP.

Infrasonic records may thus be useful for estimating mass flux and cumulative mass flux produced during an eruption (Fig. 3). Cumulative mass flux is a crucial parameter to recover because it is closely related to the bulk gas emissions, a primary factor for characterization of eruption magnitude. However, several approximations must be considered when estimating mass flux values: (1) instrument response and propagation effects are deconvolved, (2) wind noise and barometric changes are negligible, (3) the acoustic source is a point location fixed at the vent, (4) pressure pertubations at the source are small enough that a linear relationship exists between excess pressure, particle velocity, and particle displacement. From a recorded acoustic pressure trace, the corresponding mass flux (kg/s) for a source of a time duration (τ) may be approximated by:

$$q(\tau) = 2\pi r \int_0^\tau \Delta P\left(t + \frac{r}{c}\right) dt \qquad (7)$$

In theory, the cumulative gas outflow ($M(t)$) is then the time integral of the mass flux rate:

$$M(t) = \int_0^\tau 2\pi r \left[\int_0^\tau \Delta P\left(t + \frac{r}{c}\right) dt \right] d\tau \qquad (8)$$

Unfortunately, low-frequency contributions to the cumulative mass flux are often inadequately represented because excess pressure signals are the time derivative of mass flux. In other words, laminar, steady-state gas flow out of a vent should theoretically generate no infrasound. Because passive degassing is a common mechanism at most active volcanoes (Sparks, 1998), cumulative gas flux values recovered from infrasonic pressure records should be strictly considered a lower limit, or an estimate of a transient contribution. It is also important to note that excess infrasonic pressure amplitudes are not proportional to mass flux for larger eruption plumes. A diffuse source region with a dimension comparable to infrasonic wavelengths (17 m for 20 Hz to 340 m for 1 Hz) will produce infrasonic energy that can combine destructively.

In certain situations, cumulative mass flux estimates may still be useful. The onset of most Strombolian explosions are naturally impulsive. Because gas expansion accelerates dramatically at the onset of a Strombolian explosion, high-amplitude infrasonic excess pressures are often generated. These impulses may be used to determine a cumulative mass outflow for the onset of an explosion. A comparison of gas flux estimates
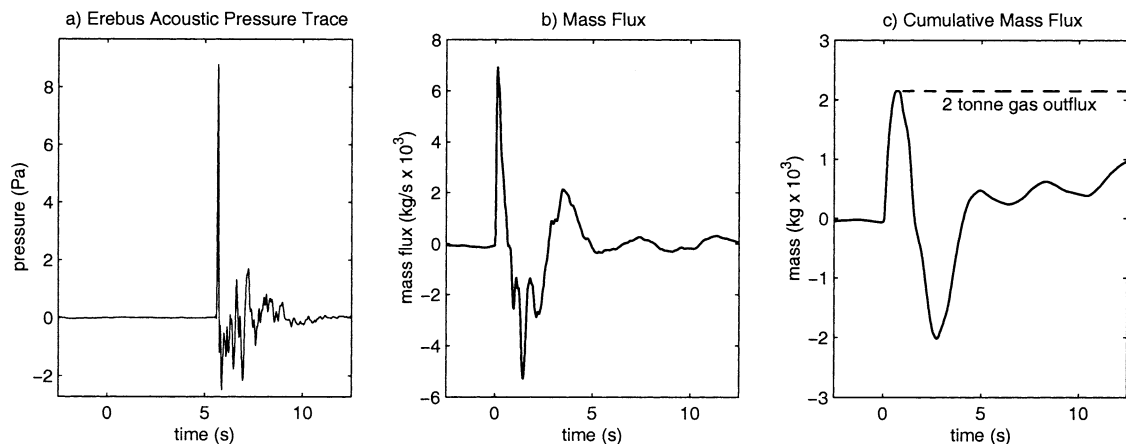
Fig. 3. Infrasonic pulse and associated mass flux. (a) Recorded acoustic pressure trace associated with an explosion at Erebus (1999:359:06:52), recorded 660 m from the vent. The example is selected because it is a low-noise, simple explosion. (b) Corresponding mass flux time history according to Eq. 7. (c) Cumulative gas flux according to Eq. 8. Dashed line represents maximum mass outflux. Negative mass fluxes are likely artificial, low-frequency artifacts due to an inadequate low-frequency response of the microphone.

for Strombolian explosions at Karymsky Volcano is determined through simultaneous analysis of infrasound records and video by Johnson (2000).

The presence of high-amplitude atmospheric pressure waves allows quick and unequivocal differentiation between subsurface seismicity (B-type earthquakes) and the seismicity associated with gas release from a vent (explosion earthquakes). However arrays of infrasonic microphones are also extremely valuable for pinpointing a volcanic seismo-acoustic source. An explosion source can be very accurately located by examination of infrasonic arrivals which tend to be impulsive and possess self-similar waveforms across an array (Fig. 4). In contrast, it is often very difficult to even identify the compressional phase from low-frequency explosion earthquakes (Johnson and Lees, 2000). Furthermore, acoustic propagation velocities in the atmosphere are an order of magnitude slower than seismic velocities in the earth. For arrays deployed at intermediate epicentral distances (within 5 km of the vent), explosion sources can be located with only a few meters error. The location of an explosion source is particularly important for volcanic systems which possess multiple active vents such as Stromboli (Ripepe et al., 2001).

4. Infrasound propagation in the atmosphere

Though the elastic structure of the atmosphere is much less complicated than that of the earth, acoustic energy is still bent and refracted by velocity and wind gradients. In certain instances, acoustic shadow zones are possible at distances more than a few kilometers from the source. Under suitable conditions (such as during the 1883 Krakatoa eruption), acoustic signals may be ducted in low-velocity sound channels and remain audible at distances of many thousands of kilometers (Bedard and Georges, 2000). Eyewitness reports of sounds heard from large eruptions may be mapped regionally (Fairfield, 1980; Power, 1993) to reveal zones of inaudibility (often close to the volcano or upwind of the volcano) and zones of high sound intensity (sometimes several hundred kilometers from the vent). Johnson and Malone (1997) explain the audibility patterns from the 1980 Mount St. Helens airblast by tracing acoustic rays in a US standard atmosphere (Fig. 5). They utilize Garces et al.'s (1998) formulation for computing traveltimes of infrasonic waves propagating in a stratified atmosphere where a wind and temperature-dependent ray parameter (p) is conserved:
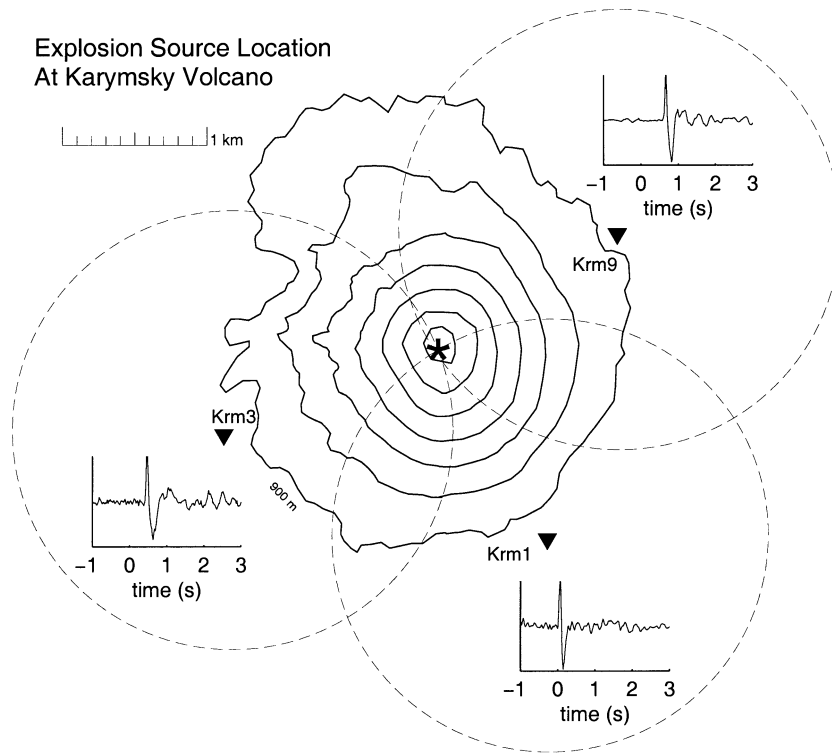
Fig. 4. Vent location determined from acoustic arrivals across an infrasound array. Microphone arrays at Karymsky Volcano can be used to accurately pinpoint the vent because infrasonic signals are impulsive and acoustic velocities are relatively slow. In this example, the 3-D source location is confined to the 2-D surface of the volcanic edifice.

$$p = \frac{\sin(i_o)}{c(z)}\left(1 + \frac{u(z)\sin(i_o)}{c(z)}\right)^{-1} \qquad (9)$$

where i_o is the angle of incidence (from vertical); $c(z)$ is the temperature-dependent intrinsic sound speed; and $u(z)$ is the horizontal wind speed (parallel to propagation direction).

Even at the intermediate distances of 100 m to 5 km commonly cited during the deployment of microphones at Strombolian-type volcanoes, atmospheric structure may influence the amplitude of a recorded infrasonic pressure trace. Fig. 6 presents several potential weather scenarios, the corresponding acoustic raypaths for those weather conditions, and effective excess pressure magnification factors calculated from traveltime curves. The magnification factor (MF) is defined here as the square root of the ratio of the recorded pressure amplitude to the expected pressure amplitude for an isotropic acoustic source radiating spherically into a homogenous atmosphere:

$$MF(X) = \sqrt{\frac{Ed_{\text{structured}}}{Ed_{\text{homogeneous}}}} \qquad (10)$$

The energy density (Ed) is defined by (Lay and Wallace, 1995):

$$Ed = \frac{\tan(i_o)}{X\cos(i_1)}\frac{dp}{dX} \qquad (11)$$

where i_1 is the incidence raypath angle (from vertical) and X is the horizontal distance from source.

Under conditions of low wind and reasonable temperature gradients, magnification factors less than a factor of two should be expected out to distances of about 5 km. But beyond these distances, magnification factors often change dramatically. Upward refraction of acoustic energy can create silent zones relatively close to the source (Fig. 6c,d). In general, wind rather than temperature gradient appears to have a more substantial influence upon magnification factors.
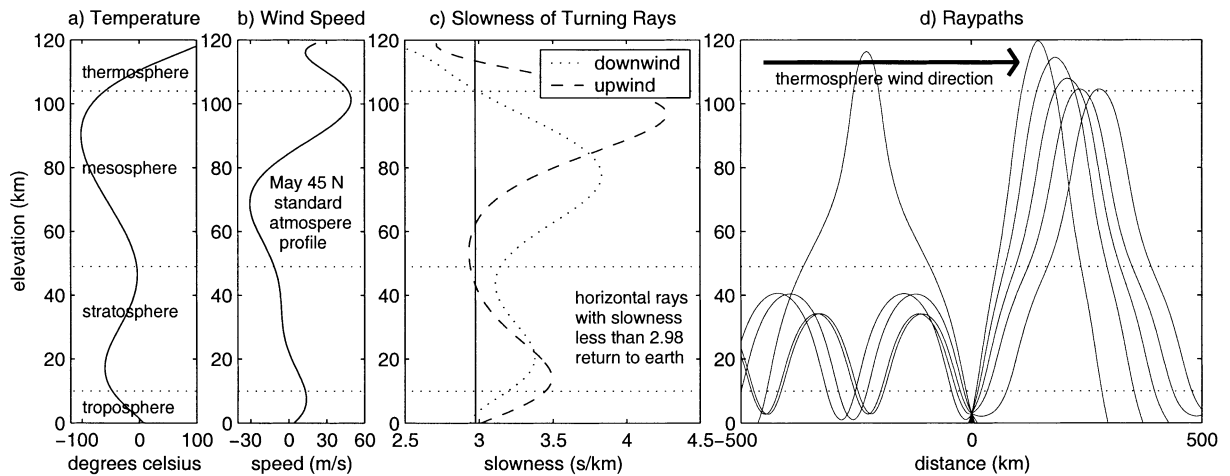
Fig. 5. Regional infrasound propagation. (a) Temperature profile, (b) zonal wind profile, and (c) horizontal ray parameter profile (according to Eq. 9) for the month of May at 45° north. (d) Acoustic raypaths from an explosion source such as the May 18, 1980, Mount St. Helens blast are refracted in the stratosphere and thermosphere. Rays are drawn at 10° increments. Illustration reproduced from Johnson and Malone (1997).

Under windy conditions, or under drastic temperature gradients, shadow zones may be found at distances as close as 2 km from the source.

Apart from geometric spreading, some acoustic attenuation results from propagation inefficiencies through the atmosphere due to molecular absorption and viscous friction losses as well as scattering, reflection, and absorption effects at boundaries. In classical acoustic attenuation, amplitude decay due to transmission losses through the atmosphere depends exponentially upon the square of the frequency (Reed, 1972):

$$\Delta P = \Delta P_i e^{-(\alpha f^2/\rho_a)r} \qquad (12)$$

in which ΔP_i is the initial overpressure; α is the attenuation coefficient; and f is the frequency (Hz).

According to Reed (1972), empirical values for α/ρ_a range from 1.3×10^{-11} s²/m to 3.0×10^{-11} s²/m which translate to about 2×10^{-5} dB/km for 10 Hz infrasound. These small values hint that attenuation of infrasound is nearly insignificant in the lower atmosphere even at global distances. However, other investigators argue that the attenuation coefficient (α) depends significantly upon atmospheric moisture content and acoustic frequency. Though few attenuation experiments are conducted in the infrasonic bandwidth, Bass and Bauer (1972) cite absorption coefficients as high as 2×10^{-1} dB/km for 10 Hz infrasound in dry air and 2×10^{-3} dB/km in air with 100% humidity.

Scattering and reflections due to wind turbulence or localized density contrasts (such as an ash cloud) are other mechanisms which should be considered and may be responsible for acoustic energy dissipation. Such atmospheric heterogeneities can have pronounced effects upon higher frequency acoustic waves, but may not be significant for infrasonic energy with relatively long quarter wavelengths (ranging from 4 m at 20 Hz to 85 m at 1 Hz). Frequency dependence is also an important consideration when evaluating the site response of a microphone. Barriers or topography in the vicinity of a recording site may preferentially filter out higher frequencies. Maekawa (1968) shows that the loss of signal amplitude is roughly proportional to the ratio of the barrier height over the acoustic wavelength.

5. Non-linear propagation and explosive shocks

For very large volcanic explosion sources and/or in the near-field, the propagation of acoustic airwaves may be non-linear because initial mass flux is either supersonic or pressure transients are
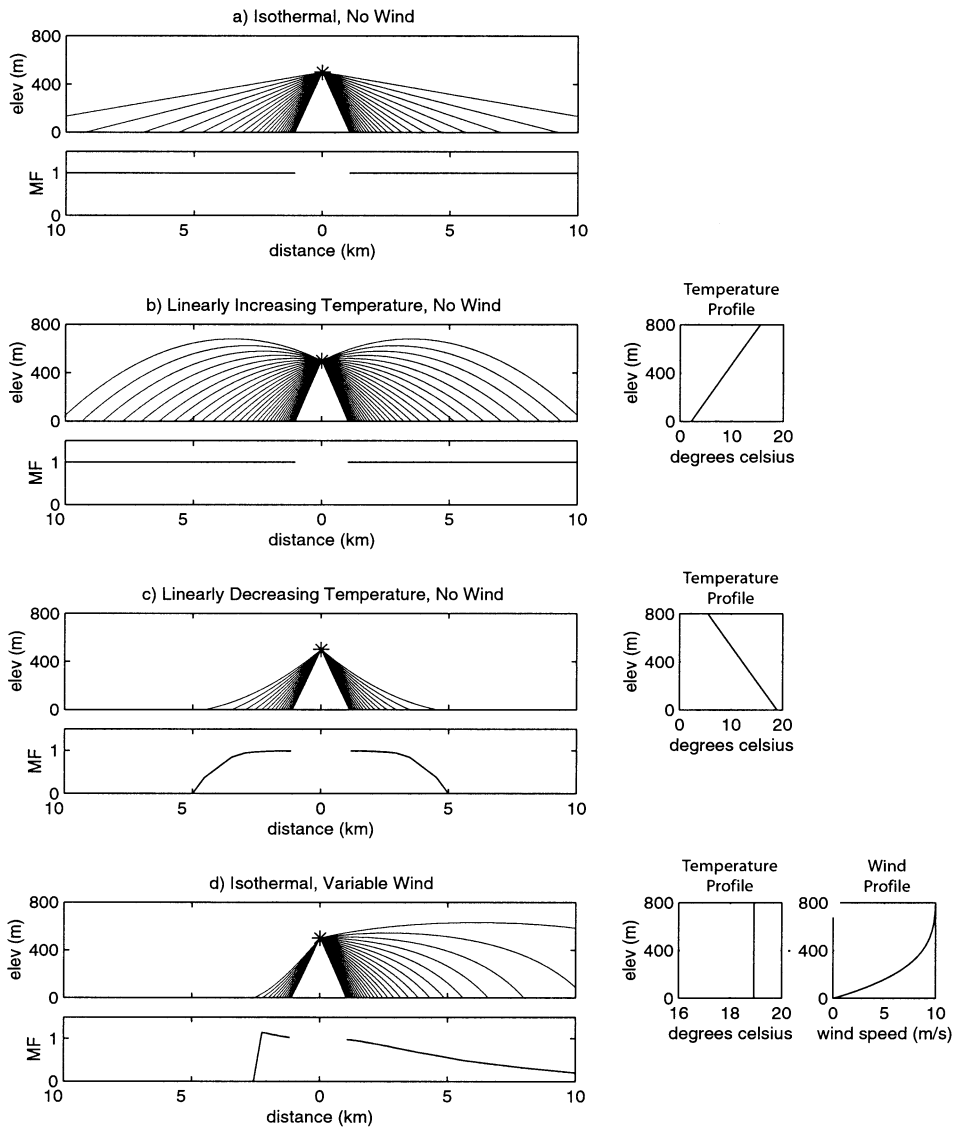
Fig. 6. Infrasound focusing at close offsets. Dependence of raypaths on variable atmospheric conditions: (a) homogeneous temperature structure with no wind, (b) temperature inversion with no wind, (c) normal temperature gradient with no wind, and (d) isothermal atmosphere and wind increasing with altitude. Acoustic rays are drawn at 1° increments. Magnification factors (MF) for each raypath are shown for the four scenarios. An absence of raypaths impacting the ground constitutes a shadow zone.

high enough that the linear acoustic approximation is invalid. Chemical explosions generate non-linear shock waves (discontinuous pressure traces) by expanding at supersonic velocities. Although Strombolian ejection velocities range up to only a few hundred meters per second (Sparks, 1997), there is evidence for Plinian eruptions with emissions exceeding 500 m/s (Wilson, 1980). Shock wave velocities exceed sound speed as a function of the shock excess pressure (Kinney and Graham, 1985):

$$\overline{M} = \sqrt{1 + \left(\frac{\gamma + 1}{2\gamma}\right)\left(\frac{\Delta P}{P_o}\right)} \qquad (13)$$

where $\overline{M}$ is the Mach number = (shock speed)/(sound speed).

As a shock wave expands radially, excess pressure drops and Mach number decreases until the shock wave decays into acoustic waves that travel at ambient sound speed. Arrival times for shock waves propagating to far offsets can be predicted by integrating along slowness/distance curves. A spherical shock with 0.01 bar excess pressure at 1 km will precede a low amplitude acoustic wave by approximately 0.13 s at far offsets. And a shock wave with 0.1 bar excess pressure at 1 km will arrive 1.3 s faster than a low amplitude acoustic wave. Though excess pressure from large eruptions may exceed 0.01 bar ($\sim 10^3$ Pa) at distances of 1 km (Reed, 1987), upper bounds for excess pressures from Strombolian explosions are approximately 10^2 Pa at 1 km. Airwaves from Strombolian explosions thus propagate very close to the speed of sound.

Even when volcanic muzzle velocities are initially subsonic, pressure pertubations may be large enough that acoustic signals steepen or 'shock up' with time (Kinney and Graham, 1985) producing a non-linear Green's function. As acoustic pressure pertubations propagate, the atmosphere heats or cools adiabatically. Because sound speed increases with the square root of temperature, trailing portions of an acoustic pressure wave with large excess pressures can catch up toward the front of the acoustic wave. This mechanism is employed by Reed (1987) to explain how low-frequency air waves that were inaudible within 50 km of the Mount St. Helens eruption acquired higher audible frequencies at farther offsets.

As a first order approximation for ideal gases under adiabatic conditions, sound speed can be related to excess pressure (see Appendix) by:

$$\Delta c = c \left[\left(\frac{P_o + \Delta P}{P_o} \right)^{\frac{\gamma-1}{2\gamma}} - 1 \right] \qquad (14)$$

in which Δc is the change in sound speed.

Fig. 7 illustrates the potential transformation of different amplitude pressure waves according to Eq. 14. Although the waveform modeling is simplistic, it gives an indication of excess pressure amplitudes where non-linear effects may become important and pressure wavefronts can steepen.

Airwaves generated by Strombolian explosions will not 'shock up' because excess pressures are too low. However, large Plinian eruptions may be capable of generating pressure-time traces which evolve as they propagate away from the source.

6. Summary

In recent years, the co-installation of low-frequency acoustic pressure sensors at seismic sites has significantly furthered the understanding of volcanic explosion dynamics. Erupting volcanoes generate substantial energy in the infrasonic bandwidth (below 20 Hz), a portion of the acoustic spectrum that suffers very little attenuation due to transmission losses and receiver site response. Unlike seismic radiation, infrasound provides a relatively unfiltered version of source motions at the vent because shear waves do not exist in the atmosphere and large, small-scale velocity gradients are uncommon. Reflections, scattering, dispersion, and attenuation within the atmosphere thus do not usually have pronounced effect on infrasonic waveforms. Unfortunately, acoustic propagation in the atmosphere is influenced by time-varying atmospheric conditions which can cause acoustic energy to refract and either focus or defocus. To accurately recover pressure time histories at the vent, care must be taken to understand the propagation effects caused by changeable atmospheric winds and temperatures. For infrasonic microphones located at intermediate epicentral distances (within 5 km of the vent), these effects are generally small. Excess pressure time histories recovered for an explosion source are proportional to the time derivative of the mass flux. For many explosions, infrasound strength is a good measure of the impulsivity of the degassing source. For very large explosions (excess pressures greater than $\sim 10^3$ Pa at 1 km), the acoustic approximation is not appropriate because excess pressures are large enough that an explosion begins as or becomes a shock wave. However, these excess pressures are not likely exceeded during Strombolian volcanism.
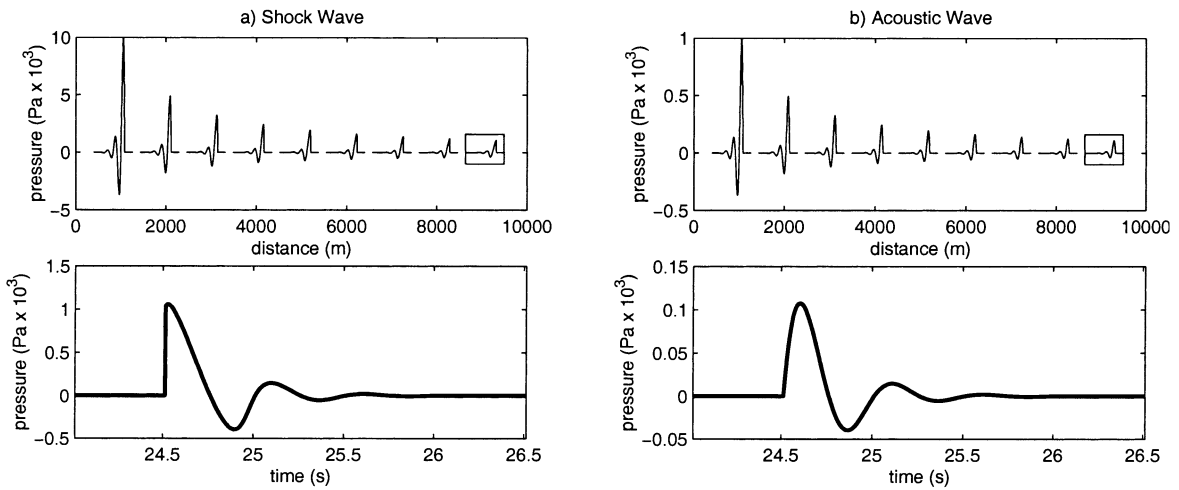
Fig. 7. Non-linear infrasound propagation. (a) Pressure-distance waveform evolution for a 2-Hz damped sinusoid with 0.1 bar maximum excess pressure at 1000 m epicentral distance (possible excess pressure generated during a Plinian event). (b) Pressure-distance waveform evolution for a 2-Hz damped sinusoid with 0.01 bar maximum excess pressure at 1000 m (very large Strombolian explosion). Waveforms are modeled at STP according to Eq. 14, assuming hemispherical spreading and no attenuation. Lower panels show pressure-time waveforms at 9 km. Shocking-up is evident only in the larger event.

Appendix

Equation 2. The total energy contained in an acoustic wavefield is a combination of the kinetic energy associated with particle motion and the potential energy associated with elasticity. Ford (1970) provides a formula for energy density of an acoustic airwave:

$$D(x,t) = \frac{\Delta P^2}{\rho_a c^2}$$

The total acoustic energy contained in a hemispherically radiating infrasonic wave is then calculated by integrating over a volumetric halfspace:

$$E_{\text{acoustic}} = \int D(x,t)dV = 2\pi \int_0^\infty D(R,t)R^2 dR =$$

$$2\pi \int_0^\infty \left(\frac{\Delta P(R,t)^2}{\rho_a c^2} \right) R^2 dR$$

Since $\Delta P(R,t)R = \Delta P(r, t-(R-r)/c)r$ for a radially expanding acoustic wave (Ford, 1970), acoustic energy can be rewritten as:

$$E_{\text{acoustic}} = \frac{2\pi r^2}{\rho_a c^2} \int_0^\infty \Delta P \left(r, t - \frac{(R-r)}{c} \right)^2 dR$$

The radial increment dR at a fixed distance is equal to cdt, yielding:

$$E_{\text{acoustic}} = \frac{2\pi r^2}{\rho_a c} \int \Delta P(t)^2 dt$$

Equation 14. The ideal gas law ($PV = nRT$) can be rewritten in the form:

$$(PV^\gamma)P^{\gamma-1} = (nRT)^\gamma$$

which leads to the relationship:

$$\frac{(PV^\gamma)P^{\gamma-1}}{(P_o V_o^\gamma)P_o^{\gamma-1}} = \frac{(nRT)^\gamma}{(nRT_o)^\gamma}$$

Rewriting in terms of sound speed ($c^2/c_o^2 = T/T_o$ from Eq. 5) and assuming adiabatic expansion of gases ($PV^\gamma = P_o V_o^\gamma$ (Kinney and Graham, 1985) gives:

$$\frac{P^{\gamma-1}}{P_o^{\gamma-1}} = \frac{c^{2\gamma}}{c_o^{2\gamma}} \Rightarrow \frac{c}{c_o} = \left(\frac{P}{P_o} \right)^{\frac{\gamma-1}{2\gamma}}$$

Defining Δc as the difference between sound speed at excess pressure (ΔP) and ambient sound speed leads to:

$$\Delta c = c_o \left[\left(\frac{P_o + \Delta P}{P_o} \right)^{\frac{\gamma-1}{2\gamma}} - 1 \right]$$

References

Bass, H.E., Bauer, H.J., 1972. Atmospheric absorption of Sound: Analytical expressions. J. Acoust. Soc. Am. 52, 821–825.

Bedard, A.J., Georges, T.M., 2000. Atmospheric infrasound. Phys. Today 53, 32–37.

Beer, T., 1974. Atmospheric Waves. Wiley, New York, 300 pp.

Fairfield, C., 1980. OMSI sound project; the acoustic effects of the Mount St. Helens eruption on May 18, 1980. Or. Geol. 42, 200–202.

Firstov, P.P., Kravchenko, N.M., 1996. Estimation of the amount of explosive gas released in volcanic eruptions using air waves. Volcanol. Seismol. 17, 547–560.

Ford, R.D., 1970. Introduction to Acoustics. Elsevier, New York, 154 pp.

Garces, M.A., Hansen, R.A., Lindquist, K., 1998. Traveltimes for infrasonic waves propagating in a stratified atmosphere. Geophys. J. Int. 135, 255–263.

Garces, M.A., Iguchi, M., Ishihara, K., Morrissey, M.Sudo,Y., Tsutsui, T., 1999. Infrasonic precursors to a vulcanian eruption at Sakurajima Volcano, Japan. Geophys. Res. Lett. 26, 2537–2540.

Garces, M.A., McNutt, S.R., 1997. Theory of the airborne sound field generated in a resonant magma conduit. J. Volcanol. Geotherm. Res. 78, 155–178.

Hagerty, M., Schwartz, S.Y., Garces, M., Protti, M., 2000. Analysis of seismic and acoustic observations at Arenal Volcano, Costa Rica, 1995–1997. J. Volcanol. Geotherm. Res. 101, 27–65.

Jensen, F.B., Kuperman, W.A., Porter, M.B., Schmidt, H., 1994. Computational Ocean Acoustics. AIP Press, New York, 612 pp.

Johnson, J.B., 2000. Interpretation of infrasound generated by erupting volcanoes and seismo-acoustic energy partitioning during Strombolian explosions. Ph.D. Thesis, University of Washington, Seattle.

Johnson, J.B., Aster, R.C., Ruiz, M.C., Malone, S.D., McChesney, P.J., Lees, J.M., Kyle, P.R., in press. Interpretation and utility of infrasonic records from erupting volcanoes. J. Volcanol. Geotherm. Res. S0377-0273(02)00409-2, this issue.

Johnson, J.B., Lees, J.M., 2000. Plugs and chugs – Seismic and acoustic observations of degassing explosions at Karymsky, Russia and Sangay, Ecuador. J. Volcanol. Geotherm. Res. 101, 67–82.

Johnson, J.B., Malone, S.D., 1997. Acoustic Air-wave Propagation from the 1980 Mount St. Helens Eruption. Eos Trans., Am. Geophys. Union, 78(46), Fall Meeting Suppl., F130.

Kinney, G.F., Graham, K.J., 1985. Explosive Shocks in Air. Springer-Verlag, New York, 269 pp.

Lay, T., Wallace, T., 1995. Modern Global Seismology. Academic Press, San Diego, 521 pp.

Lighthill, M.J., 1978. Waves in Fluids. Cambridge University Press, New York, 504 pp.

Maekawa, Z., 1968. Noise reduction by screens. Appl. Acoust. 1, 157–173.

McGetchin, T.R., Chouet, B.A., 1979. Energy budget of the Volcano Stromboli. Geophys. Res. Lett. 6, 317–320.

Mikumo, T., Bolt, B.A., 1985. Excitation mechanism of atmospheric pressure waves from the 1980 Mount St. Helens eruption. Geophys. J. R. Astron. Soc. 81, 445–461.

Newhall, C.G., Self, S., 1982. The volcanic explosivity index (VEI): An estimate of explosive magnitude for historical volcanism. J. Geophys. Res. 87, 1231–1238.

Power, J., 1993. Sounds during the August 18, 1992, Spurr Eruption. Alsk. Volcano Obs. Newslett. 5, 14–15.

Reed, J.W., 1987. Air pressure waves from Mount St. Helens eruptions. J. Geophys. Res. 92, 11979–11982.

Reed, J.W., 1972. Attenuation of blast waves by the atmosphere. J. Geophys. Res. 77, 1616–1622.

Richards, A.F., 1963. Volcanic sounds: Investigation and analysis. J. Geophys. Res. 68, 919–928.

Ripepe, M., Ciliberto, S., Schiava, M.D., 2001. Time constraints for modeling source dynamics of volcanic explosions at Stromboli. J. Geophys. Res. 106, 8713–8727.

Rowe, C.A., Aster, R.C., Kyle, P.R., Dibble, R.R., Schlue, J.W., 2000. Seismic and acoustic observations at Mount Erebus Volcano, Ross Island, Antarctica, 1994–1998. J. Volcanol. Geotherm. Res. 101, 105–128.

Sparks, R.S.J., 1997. Volcanic Plumes. Wiley, New York, 574 pp.

Sparks, R.S.J., 1998. The Physics of Explosive Volcanic Eruptions. Geol. Soc., London, 186 pp.

Tahira, M., Nomura, M., Sawada, Y., Kamo, K., 1996. Infrasonic and acoustic-gravity waves generated by the Mount Pinatubo eruption of June 15, 1991. Fire and Mud. University of Washington Press, Seattle, pp. 601–614.

Truax, B., 1978. The World Soundscape Project's Handbook for Acoustic Ecology. A.R.C. Publications, Vancouver, 171 pp.

Vergniolle, S., Brandeis, G., Mareschal, J.-C., 1996. Strombolian explosions 2. Eruption dynamics determined from acoustic measurements. Journal of Geophysical Research 101, 20449–20466.

Wilson, L., 1980. Relationship between pressure, volatile content, and ejecta velocity in three types of volcanic explosion. J. Volcanol. Geotherm. Res. 8, 297–313.

Wilson, L., Sparks, R.S.J., Huang, T.C., Watkins, N.D., 1978. The control of volcanic column heights by eruption energetics and dynamics. J. Geophys. Res. 83, 1829–1836.

Yamasato, H., 1997. Quantitative analysis of pyroclastic flows using infrasonic and seismic data at Unzen Volcano, Japan. J. Phys. Earth 45, 397–416.

Yamasato, H., 1998. Nature of infrasonic pulse accompanying low frequency earthquake at Unzen Volcano, Japan. Bull. Volcanol. Soc. Jpn. 43, 1–13.